The analytical $\pi\pi$ scattering amplitude and the light scalars

N.N. Achasov[a] and A.V. Kiselev[a,b]

[a] *Laboratory of Theoretical Physics, Sobolev Institute for Mathematics, 630090, Novosibirsk, Russia*

[b] *Novosibirsk State University, 630090, Novosibirsk, Russia*

(Dated: November 22, 2010)

Abstract

In this work we construct the $\pi\pi$ scattering amplitude T_0^0 with regular analytical properties in the s complex plane, that describes simultaneously the data on the $\pi\pi$ scattering, $\phi \to \pi^0\pi^0\gamma$ decay and $\pi\pi \to K\bar{K}$ reaction. The chiral shielding of the $\sigma(600)$ meson and its mixing with the $f_0(980)$ meson are taken into account also. The data agrees with the four-quark nature of the $\sigma(600)$ and $f_0(980)$ mesons.

The amplitude in the range $-5m_\pi^2 < s < 0.64$ GeV^2 also agrees with results, obtained on the base of the chiral expansion, dispersion relations and the Roy equations.

PACS numbers: 12.39.-x 13.40.Hq 13.66.Bc

I. INTRODUCTION

Study of light scalar resonances is one of the central problems of non-perturbative QCD, it is important for understanding both the confinement physics and the chiral symmetry realization way in the low energy region. The commonly suggested nonet of light scalar mesons is $f_0(600)$ (or $\sigma(600)$), $K_0^*(800)$ (or $\kappa(800)$), $f_0(980)$ and $a_0(980)$ [1]. Light scalar mesons are intensively studied theoretically and experimentally in different reactions.

In Refs. [2] we described the high-statistical KLOE data on the $\phi \to \pi^0\pi^0\gamma$ decay [3] simultaneously with the data on the $\pi\pi$ scattering and the $\pi\pi \to K\bar{K}$ reaction. The description was carried out taking into account the chiral shielding of the $\sigma(600)$ meson [4, 5] and it's mixing with the $f_0(980)$ meson. It was shown that the data don't contradict the existence of the $\sigma(600)$ meson and yield evidence in favor of the four-quark nature of the $\sigma(600)$ and $f_0(980)$ mesons.

This description revealed new goals. The point is that at the same time it was calculated in Ref. [6] the $\pi\pi$ scattering amplitude in the s complex plane, basing on chiral expansion, dispersion relations and Roy equations. In particular, the pole was obtained at $s = M_\sigma^2 = (6.2 - 12.3i)\, m_\pi^2$, where

$$M_\sigma = 441^{+16}_{-8} - i272^{+9}_{-12.5}\ \text{MeV}\,, \tag{1}$$

that was assigned to the σ resonance.

Aiming the comparison of the results of Refs. [2] and [6] it is necessary to build the $\pi\pi$ scattering amplitude with correct analytical properties in the complex s plane. The point is that in Ref. [2] S-matrix of the $\pi\pi$ scattering is the product of the "resonance" and "background" parts:

$$S_{\pi\pi} = S_{back}\, S_{res}\,, \tag{2}$$

and the S_{res} had correct analytical properties, while analytical properties of the S_{back} in the whole complex s plane were not essential for the aims of [2], where physical region was investigated, and Adler zero existence [7] together with poles absence on the real axis of the s complex plane were demanded.

In this paper we present the $\pi\pi$ scattering amplitude with correct analytical properties in the complex s plane and the data description obtained with this amplitude [8]. The

comparison with the results of Ref. [6] is presented also.

All formulas for the $\phi \to (S\gamma + \rho^0\pi^0) \to \pi^0\pi^0\gamma$ reaction ($S = f_0(980) + \sigma(600)$) are shown in Sec. II. Our new parameterization of the background amplitude is presented in Sec. III and Sec. IV. The results of the data analysis are presented in Sec.V. A brief summary is given in Sec.VI.

II. THEORETICAL DESCRIPTION OF THE $\phi \to (f_0(980) + \sigma(600))\gamma \to \gamma\pi^0\pi^0$ AND $\phi \to \rho^0\pi^0 \to \gamma\pi^0\pi^0$ REACTIONS

In Refs. [9, 10] it was shown that the dominant background process is $\phi \to \pi^0\rho \to \gamma\pi^0\pi^0$, while the reactions $e^+e^- \to \rho \to \pi^0\omega \to \gamma\pi^0\pi^0$ and $e^+e^- \to \omega \to \pi^0\rho \to \gamma\pi^0\pi^0$ have a small effect on $e^+e^- \to \phi \to \gamma\pi^0\pi^0$ in the region $m_{\pi^0\pi^0} \equiv m > 900$ MeV. In Ref. [11] it was shown that the $\phi \to \pi^0\rho \to \gamma\pi^0\pi^0$ background is small in comparison with the signal $\phi \to \gamma f_0(980) \to \gamma\pi^0\pi^0$ at $m > 700$ MeV.

The amplitude of the background decay $\phi(p) \to \pi^0\rho \to \gamma(q)\pi^0(k_1)\pi^0(k_2)$ has the following form:

$$M_{back} = F_b e^{-i\delta} g_{\rho\pi^0\phi} g_{\rho\pi^0\gamma} \phi_\alpha p_\nu \epsilon_\delta q_\epsilon \epsilon_{\alpha\beta\mu\nu} \epsilon_{\beta\delta\omega\epsilon} \Big(\frac{k_{1\mu} k_{2\omega}}{D_\rho(q+k_2)} + \frac{k_{2\mu} k_{1\omega}}{D_\rho(q+k_1)} \Big). \tag{3}$$

Here constants F_b and δ take into account $\rho\pi$ rescattering effects [12]. Note that in this work and our previous works it was assumed that $F_b = 1$ [13].

In the K^+K^- loop model, $\phi \to K^+K^- \to \gamma(f_0 + \sigma)$ [9–11], above the $K\bar{K}$ threshold the amplitude of the signal $\phi \to \gamma(f_0 + \sigma) \to \gamma\pi^0\pi^0$ is

$$M_{sig} = g(m) \Big((\phi\epsilon) - \frac{(\phi q)(\epsilon p)}{(pq)} \Big) T\left(K^+K^- \to \pi^0\pi^0\right) \times 16\pi \,, \tag{4}$$

where the $K^+K^- \to \pi^0\pi^0$ amplitude, taking into account the mixing of f_0 and σ mesons,

$$T\left(K^+K^- \to \pi^0\pi^0\right) = e^{i\delta_B} \sum_{R,R'} \frac{g_{RK^+K^-} G^{-1}_{RR'} g_{R'\pi^0\pi^0}}{16\pi} \,, \tag{5}$$

where $R, R' = f_0, \sigma$,

$$\delta_B = \delta_B^{\pi\pi} + \delta_B^{K\bar{K}} \,, \tag{6}$$

where $\delta_B^{\pi\pi}$ and $\delta_B^{K\bar{K}}$ are phases of the elastic background of the $\pi\pi$ and $K\bar{K}$ scattering, respectively, see Refs. [14–17].

Note that the additional phase $\delta_B^{K\bar{K}}$ changes the modulus of the $K\bar{K} \to \pi^0\pi^0$ amplitude under the $K\bar{K}$ threshold, at $m < 2m_K$. Let's define

$$P_K = \begin{cases} e^{i\delta_B^{K\bar{K}}} & m \geq 2m_K\,; \\ \text{analytical continuation of } e^{i\delta_B^{K\bar{K}}} & m < 2m_K\,. \end{cases} \tag{7}$$

Note also that the phase $\delta_B^{\pi\pi}$ was defined as δ_B in Refs. [10, 11].

The matrix of the inverse propagators [10] is

$$G_{RR'} \equiv G_{RR'}(m) = \begin{pmatrix} D_{f_0}(m) & -\Pi_{f_0\sigma}(m) \\ -\Pi_{f_0\sigma}(m) & D_\sigma(m) \end{pmatrix},$$

$$\Pi_{f_0\sigma}(m) = \sum_{a,b} \frac{g_{\sigma ab}}{g_{f_0 ab}} \Pi_{f_0}^{ab}(m) + C_{f_0\sigma},$$

where the constant $C_{f_0\sigma}$ incorporates the subtraction constant for the transition $f_0(980) \to (0^-0^-) \to \sigma(600)$ and effectively takes into account contribution of multi-particle intermediate states to $f_0 \leftrightarrow \sigma$ transition, see Ref. [10]. The inverse propagator of the R scalar meson is presented also in Refs. [9–11, 14–23]:

$$D_R(m) = m_R^2 - m^2 + \sum_{ab} [Re\Pi_R^{ab}(m_R^2) - \Pi_R^{ab}(m^2)], \tag{8}$$

where $\sum_{ab}[Re\Pi_R^{ab}(m_R^2) - \Pi_R^{ab}(m^2)] = Re\Pi_R(m_R^2) - \Pi_R(m^2)$ takes into account the finite width corrections of the resonance which are the one loop contribution to the self-energy of the R resonance from the two-particle intermediate ab states.

For pseudoscalar a, b mesons and $m_a \geq m_b,\ m \geq m_+$ one has:

$$\Pi_R^{ab}(m^2) = \frac{g_{Rab}^2}{16\pi} \left[\frac{m_+ m_-}{\pi m^2} \ln \frac{m_b}{m_a} + \right.$$
$$\left. + \rho_{ab} \left(i + \frac{1}{\pi} \ln \frac{\sqrt{m^2 - m_-^2} - \sqrt{m^2 - m_+^2}}{\sqrt{m^2 - m_-^2} + \sqrt{m^2 - m_+^2}} \right) \right] \tag{9}$$

$m_- \leq m < m_+$

$$\Pi_R^{ab}(m^2) = \frac{g_{Rab}^2}{16\pi} \left[\frac{m_+ m_-}{\pi m^2} \ln \frac{m_b}{m_a} - |\rho_{ab}(m)| + \right.$$
$$\left. + \frac{2}{\pi} |\rho_{ab}(m)| \arctan \frac{\sqrt{m_+^2 - m^2}}{\sqrt{m^2 - m_-^2}} \right]. \tag{10}$$

$m < m_-$

$$\Pi_R^{ab}(m^2) = \frac{g_{Rab}^2}{16\pi}\left[\frac{m_+m_-}{\pi m^2}\ln\frac{m_b}{m_a} - \right.$$
$$\left. -\frac{1}{\pi}\rho_{ab}(m)\ln\frac{\sqrt{m_+^2-m^2}-\sqrt{m_-^2-m^2}}{\sqrt{m_+^2-m^2}+\sqrt{m_-^2-m^2}}\right]. \qquad (11)$$

$$\rho_{ab}(m) = \sqrt{(1-\frac{m_+^2}{m^2})(1-\frac{m_-^2}{m^2})}\ , \qquad m_+ = m_a \pm m_b \qquad (12)$$

The constants g_{Rab} are related to the width

$$\Gamma_R(m) = \sum_{ab}\Gamma(R\to ab, m) = \sum_{ab}\frac{g_{Rab}^2}{16\pi m}\rho_{ab}(m). \qquad (13)$$

Note that we take into account intermediate states $\pi\pi, K\bar{K}, \eta\eta, \eta'\eta, \eta'\eta'$ in the $f_0(980)$ and $\sigma(600)$ propagators:

$$\Pi_{f_0} = \Pi_{f_0}^{\pi^+\pi^-} + \Pi_{f_0}^{\pi^0\pi^0} + \Pi_{f_0}^{K^+K^-} + \Pi_{f_0}^{K^0\bar{K}^0} + \Pi_{f_0}^{\eta\eta} + \Pi_{f_0}^{\eta'\eta} + \Pi_{f_0}^{\eta'\eta'}, \qquad (14)$$

and also for the $\sigma(600)$. We use $g_{f_0K^0\bar{K^0}} = g_{f_0K^+K^-}, g_{f_0\pi^0\pi^0} = g_{f_0\pi^+\pi^-}/\sqrt{2}$, the same for the $\sigma(600)$, too.

For other coupling constants the naive four-quark model predicts [9, 21]:

$$g_{f_0\eta\eta} = -g_{f_0\eta'\eta'} = \frac{2\sqrt{2}}{3}\,g_{f_0K^+K^-},\ g_{f_0\eta'\eta} = -\frac{\sqrt{2}}{3}\,g_{f_0K^+K^-}\ ;$$

$$g_{\sigma\eta\eta} = g_{\sigma\eta\eta'} = \frac{\sqrt{2}}{3}\,g_{\sigma\pi^+\pi^-},\ g_{\sigma\eta'\eta'} = \frac{1}{3\sqrt{2}}\,g_{\sigma\pi^+\pi^-}\ .$$

The definition of $g_{R\pi^0\pi^0}$, $g_{R\eta\eta}$, $g_{R\eta'\eta'}$ takes into account the identity of the particles. As for these relations are approximate, we introduce the effective correction coefficients x_σ and x_{f_0}:

$$g_{f_0\eta\eta} = -g_{f_0\eta'\eta'} = \frac{2\sqrt{2}}{3}\,g_{f_0K^+K^-}\,x_{f_0},\ g_{f_0\eta'\eta} = -\frac{\sqrt{2}}{3}\,g_{f_0K^+K^-}\,x_{f_0}\ ;$$

$$g_{\sigma\eta\eta} = g_{\sigma\eta\eta'} = \frac{\sqrt{2}}{3}\,g_{\sigma\pi^+\pi^-}x_\sigma,\ g_{\sigma\eta'\eta'} = \frac{1}{3\sqrt{2}}\,g_{\sigma\pi^+\pi^-}x_\sigma\ .$$

In the K^+K^- loop model $g(m)$ has the following forms (see Refs. [9, 20, 22, 23]).

For $m < 2m_{K^+}$

$$g(m) = \frac{e}{2(2\pi)^2} g_{\phi K^+K^-} \Bigg\{ 1 + \frac{1-\rho^2(m^2)}{\rho^2(m_\phi^2) - \rho^2(m^2)} \times$$
$$\Bigg[2|\rho(m^2)| \arctan \frac{1}{|\rho(m^2)|} - \rho(m_\phi^2)\lambda(m_\phi^2) + i\pi\rho(m_\phi^2) -$$
$$-(1-\rho^2(m_\phi^2)) \Bigg(\frac{1}{4}(\pi + i\lambda(m_\phi^2))^2 -$$
$$- \left(\arctan \frac{1}{|\rho(m^2)|} \right)^2 \Bigg) \Bigg] \Bigg\}, \tag{15}$$

where

$$\rho(m^2) = \sqrt{1 - \frac{4m_{K^+}^2}{m^2}} \; ; \qquad \lambda(m^2) = \ln \frac{1+\rho(m^2)}{1-\rho(m^2)} \; ; \qquad \frac{e^2}{4\pi} = \alpha = \frac{1}{137} \; . \tag{16}$$

For $m \geq 2m_{K^+}$

$$g(m) = \frac{e}{2(2\pi)^2} g_{\phi K^+K^-} \Bigg\{ 1 + \frac{1-\rho^2(m^2)}{\rho^2(m_\phi^2) - \rho^2(m^2)} \times$$
$$\times \Bigg[\rho(m^2)(\lambda(m^2) - i\pi) - \rho(m_\phi^2)(\lambda(m_\phi^2) - i\pi) -$$
$$\frac{1}{4}(1-\rho^2(m_\phi^2)) \Bigg((\pi + i\lambda(m_\phi^2))^2 - (\pi + i\lambda(m^2))^2 \Bigg) \Bigg] \Bigg\}. \tag{17}$$

The mass spectrum of the reaction is

$$\frac{\Gamma(\phi \to \pi^0\pi^0\gamma)}{dm} = \frac{d\Gamma_S}{dm} + \frac{d\Gamma_{back}(m)}{dm} + \frac{d\Gamma_{int}(m)}{dm}, \tag{18}$$

where the signal contribution $\phi \to S\gamma \to \pi^0\pi^0\gamma$

$$\frac{d\Gamma_S}{dm} = \frac{|P_K|^2 |g(m)|^2 \sqrt{m^2 - 4m_\pi^2}(m_\phi^2 - m^2)}{3(4\pi)^3 m_\phi^3} |\sum_{R,R'} g_{RK^+K^-} G^{-1}_{RR'} g_{R'\pi^0\pi^0}|^2. \tag{19}$$

The mass spectrum of the background process $\phi \to \rho\pi^0 \to \pi^0\pi^0\gamma$

$$\frac{d\Gamma_{back}(m)}{dm} = \frac{1}{2} \frac{(m_\phi^2 - m^2)\sqrt{m^2 - 4m_\pi^2}}{256\pi^3 m_\phi^3} \int_{-1}^{1} dx A_{back}(m,x) \, , \tag{20}$$

where

$$A_{back}(m,x) = \frac{1}{3} \sum |M_{back}|^2 = \tag{21}$$

$$= \frac{F_b^2}{24} g_{\phi\rho\pi}^2 g_{\rho\pi\gamma}^2 \Big\{ \Big(m_\pi^8 + 2m^2 m_\pi^4 \tilde{m}_\rho^2 - 4m_\pi^6 \tilde{m}_\rho^2 + 2m^4 \tilde{m}_\rho^4 -$$
$$-4m^2 m_\pi^2 \tilde{m}_\rho^4 + 6m_\pi^4 \tilde{m}_\rho^4 + 2m^2 \tilde{m}_\rho^6 - 4m_\pi^2 \tilde{m}_\rho^6 + \tilde{m}_\rho^8 - 2m_\pi^6 m_\phi^2 -$$
$$-2m^2 m_\pi^2 \tilde{m}_\rho^2 m_\phi^2 + 2m_\pi^4 \tilde{m}_\rho^2 m_\phi^2 - 2m^2 \tilde{m}_\rho^4 m_\phi^2 + 2m_\pi^2 \tilde{m}_\rho^4 m_\phi^2 - 2\tilde{m}_\rho^6 m_\phi^2 +$$
$$+m_\pi^4 m_\phi^4 + \tilde{m}_\rho^4 m_\phi^4 \Big) \Big(\frac{1}{|D_\rho(\tilde{m}_\rho)|^2} + \frac{1}{|D_\rho(\tilde{m}_\rho^*)|^2} \Big) + (m_\phi^2 - m^2)(m^2 -$$
$$-2m_\pi^2 + 2\tilde{m}_\rho^2 - m_\phi^2)(2m^2 m_\pi^2 + 2m_\pi^2 m_\phi^2 - m^4) \frac{1}{|D_\rho(\tilde{m}_\rho^*)|^2} +$$
$$+2\mathrm{Re} \Big(\frac{1}{D_\rho(\tilde{m}_\rho) D_\rho^*(\tilde{m}_\rho^*)} \Big) \Big(m_\pi^8 - m^6 \tilde{m}_\rho^2 + 2m^4 m_\pi^2 \tilde{m}_\rho^2 +$$
$$+2m^2 m_\pi^4 \tilde{m}_\rho^2 - 4m_\pi^6 \tilde{m}_\rho^2 - 4m^2 m_\pi^2 \tilde{m}_\rho^4 + 6m_\pi^4 \tilde{m}_\rho^4 +$$
$$+2m^2 \tilde{m}_\rho^6 - 4m_\pi^2 \tilde{m}_\rho^6 + \tilde{m}_\rho^8 + m^2 m_\pi^4 m_\phi^2 - 2m_\pi^6 m_\phi^2 + 2m^4 \tilde{m}_\rho^2 m_\phi^2 -$$
$$-4m^2 m_\pi^2 \tilde{m}_\rho^2 m_\phi^2 + 2m_\pi^4 \tilde{m}_\rho^2 m_\phi^2 - m^2 \tilde{m}_\rho^4 m_\phi^2 + 2m_\pi^2 \tilde{m}_\rho^4 m_\phi^2 - 2\tilde{m}_\rho^6 m_\phi^2 -$$
$$-m_\pi^4 m_\phi^4 - m^2 \tilde{m}_\rho^2 m_\phi^4 + 2m_\pi^2 \tilde{m}_\rho^2 m_\phi^4 + \tilde{m}_\rho^4 m_\phi^4 \Big) \Big\},$$

$$\tilde{m_\rho}^2 = m_\pi^2 + \frac{(m_\phi^2 - m^2)}{2} (1 - x\sqrt{1 - \frac{4m_\pi^2}{m^2}})$$
$$\tilde{m_\rho}^{*2} = m_\phi^2 + 2m_\pi^2 - m^2 - \tilde{m_\rho}^2 \,. \tag{22}$$

The interference between signal and background processes accounts for

$$\frac{d\Gamma_{int}(m)}{dm} = \frac{1}{\sqrt{2}} \frac{\sqrt{m^2 - 4m_\pi^2}}{256\pi^3 m_\phi^3} \int_{-1}^{1} dx A_{int}(m,x) \,, \tag{23}$$

where

$$A_{int}(m,x) = \frac{2}{3}(m_\phi^2 - m^2)\mathrm{Re} \sum M_f M_{back}^* = \tag{24}$$
$$= \frac{16\pi}{3} F_b \mathrm{Re} \Big\{ e^{i\delta} g(m) g_{\phi\rho\pi} g_{\rho\pi\gamma} T_0^0 \left(K^+ K^- \to \pi^0 \pi^0 \right) \Big[\frac{(\tilde{m}_\rho^2 - m_\pi^2)^2 m_\phi^2 - (m_\phi^2 - m^2)^2 \tilde{m}_\rho^2}{D_\rho^*(\tilde{m}_\rho)} +$$
$$+ \frac{(\tilde{m}_\rho^{*2} - m_\pi^2)^2 m_\phi^2 - (m_\phi^2 - m^2)^2 \tilde{m}_\rho^{*2}}{D_\rho^*(\tilde{m}_\rho^*)} \Big] \Big\} =$$
$$= \frac{F_b}{3} \mathrm{Re} \Big\{ P_K e^{i\delta_B^{\pi\pi}} e^{i\delta} g(m) g_{\phi\rho\pi} g_{\rho\pi^0\gamma} \Big(\sum_{R,R'} g_{RK^+K^-} G_{RR'}^{-1} g_{R'\pi^0\pi^0} \Big) \times$$
$$\times \Big[\frac{(\tilde{m}_\rho^2 - m_\pi^2)^2 m_\phi^2 - (m_\phi^2 - m^2)^2 \tilde{m}_\rho^2}{D_\rho^*(\tilde{m}_\rho)} + \frac{(\tilde{m}_\rho^{*2} - m_\pi^2)^2 m_\phi^2 - (m_\phi^2 - m^2)^2 \tilde{m}_\rho^{*2}}{D_\rho^*(\tilde{m}_\rho^*)} \Big] \Big\} .$$

The factor 1/2 in Eq. (20) and the factor $1/\sqrt{2}$ in Eq. (23) take into account the identity of pions.

The S-wave amplitude T_0^0 of the $\pi\pi$ scattering with I=0 [10, 15–17] is

$$T_0^0 = \frac{\eta_0^0 e^{2i\delta_0^0} - 1}{2i\rho_{\pi\pi}(m)} = \frac{e^{2i\delta_B^{\pi\pi}} - 1}{2i\rho_{\pi\pi}(m)} + e^{2i\delta_B^{\pi\pi}} \sum_{R,R'} \frac{g_{R\pi\pi} G^{-1}_{RR'} g_{R'\pi\pi}}{16\pi} \,. \tag{25}$$

Here $\eta_0^0 \equiv \eta_0^0(m)$ is the inelasticity, $\eta_0^0 = 1$ for $m \leq 2m_{K^+}$, and

$$\delta_0^0 \equiv \delta_0^0(m) = \delta_B^{\pi\pi}(m) + \delta_{res}(m) \,, \tag{26}$$

where $\delta_B^{\pi\pi} = \delta_B^{\pi\pi}(m)$ (δ_B in Ref. [10]) is the phase of the elastic background (see Eq. 6), and $\delta_{res}(m)$ is the resonance scattering phase,

$$S_0^{0\ res} = \eta_0^0(m) e^{2i\delta_{res}(m)} = 1 + 2i\rho_{\pi\pi}(m) \sum_{R,R'} \frac{g_{R\pi\pi} G^{-1}_{RR'} g_{R'\pi\pi}}{16\pi} \,, \;\; \eta_0^0 = |S_0^{0\ res}| \,, \tag{27}$$

$g_{R\pi\pi} = \sqrt{3/2}\, g_{R\pi^+\pi^-}$. The chiral shielding phase $\delta_B^{\pi\pi}(m)$, motivated by the σ-model [4, 5] and desired analytical properties, is taken in more complicated form than in Ref. [2], see Sec. III.

The phase $\delta_B^{K\bar{K}} = \delta_B^{K\bar{K}}(m)$ is parameterized in the following way:

$$\tan\delta_B^{K\bar{K}} = f_K(m^2)\sqrt{m^2 - 4m_{K^+}^2} \equiv 2p_K f_K(m^2) \tag{28}$$

and

$$e^{2i\delta_B^{K\bar{K}}} = \frac{1 + i2p_K f_K(m^2)}{1 - i2p_K f_K(m^2)} \tag{29}$$

Actually, $e^{2i\delta_B^{\pi\pi}(m)}$ has a pole at $m^2 = m_0^2$, $0 < m_0^2 < 4m_\pi^2$, which is compensated by the zero in $e^{2i\delta_B^{K\bar{K}}(m)}$ to ensure a regular $K\bar{K} \to \pi\pi$ amplitude and, consequently, the $\phi \to K^+K^- \to \pi\pi\gamma$ amplitude at $0 < m^2 < 4m_\pi^2$. This requirement leads to

$$f_K(m_0^2) = \frac{1}{\sqrt{4m_{K^+}^2 - m_0^2}} \approx \frac{1}{2m_{K^+}} \,. \tag{30}$$

As in Refs. [2], for $f_K(m^2)$ we used the form

$$f_K(m^2) = -\frac{\arctan(\frac{m^2 - m_1^2}{m_2^2})}{\Lambda_K} \,. \tag{31}$$

The inverse propagator of the ρ meson has the following expression

$$D_\rho(m) = m_\rho^2 - m^2 - im^2 \frac{g_{\rho\pi\pi}^2}{48\pi}\Big(1 - \frac{4m_\pi^2}{m^2}\Big)^{3/2} . \tag{32}$$

.

The coupling constants $g_{\phi K^+K^-} = 4.376 \pm 0.074$ and $g_{\phi\rho\pi} = 0.814 \pm 0.018$ GeV^{-1} are taken from the most precise measurement [24]. To obtain the coupling constant $g_{\rho\pi^0\gamma}$ we used the data of the experiments [25] and [26] on the $\rho \to \pi^0\gamma$ decay and the expression

$$\Gamma(\rho \to \pi^0\gamma) = \frac{g_{\rho\pi^0\gamma}^2}{96\pi m_\rho^3}(m_\rho^2 - m_\pi^2)^3, \tag{33}$$

the result $g_{\rho\pi^0\gamma} = 0.26 \pm 0.02$ GeV^{-1} is the weighed average of these experiments.

III. THE BACKGROUND PHASE $\delta_B^{\pi\pi}$

The proper analytical properties of the $\pi\pi$ scattering amplitude are: two cuts in the s-complex plane, Adler zero in T_0^0 [27], absence of poles on the physical sheet of the Riemannian surface, $\sigma(600)$ and $f_0(980)$ poles in the resonance amplitude on the second sheet of the Riemannian surface and absence of poles on the second sheet in the background amplitude in the region $4m_\pi^2 < \mathrm{Re}(s) < (1.2\ \mathrm{GeV})^2$. This applies curtain restrictions on the $\delta_B^{\pi\pi}$.

Let's represent $\delta_B^{\pi\pi}$ in the physical region $s = m^2 > 4m_\pi^2$ as

$$\tan(\delta_B^{\pi\pi}) = \frac{\mathrm{Im}\,(P_{\pi 1}(s)P_{\pi 2}(s))}{\mathrm{Re}\,(P_{\pi 1}(s)P_{\pi 2}(s))}\,, \tag{34}$$

and

$$e^{2i\delta_B^{\pi\pi}} = S_1^{back}S_2^{back} = \frac{P_{\pi 1}^*(s)P_{\pi 2}^*(s)}{P_{\pi 1}(s)P_{\pi 2}(s)} = \frac{P_{\pi 1}(s-i\epsilon)P_{\pi 2}(s-i\epsilon)}{P_{\pi 1}(s+i\epsilon)P_{\pi 2}(s+i\epsilon)}\,, \tag{35}$$

where

$$P_{\pi 1}(s) = a_1 - a_2\frac{s}{4m_\pi^2} - \Pi_{\pi\pi}(s) + a_3\,\Pi_{\pi\pi}(4m_\pi^2 - s) - a_4 Q_1(s)\,, \tag{36}$$

$$Q_1(s) = \frac{1}{\pi}\int_{4m_\pi^2}^{\infty}\frac{s-4m_\pi^2}{s'-4m_\pi^2}\frac{\rho_{\pi\pi}(s')}{s'-s-i\varepsilon}K_1(s')\,, \tag{37}$$

$$K_1(s) = \frac{L_1(s)}{D_1(4m_\pi^2-s)D_2(4m_\pi^2-s)D_3(4m_\pi^2-s)D_4(4m_\pi^2-s)D_5(4m_\pi^2-s)D_6(4m_\pi^2-s)}\,, \tag{38}$$

$$L_1(s) = (s-4m_\pi^2)^6 + \alpha_1(s-4m_\pi^2)^5 + \alpha_2(s-4m_\pi^2)^4 + \alpha_3(s-4m_\pi^2)^3 + \\ + \alpha_4(s-4m_\pi^2)^2 + \alpha_5(s-4m_\pi^2) + \alpha_6 + \\ + \sqrt{s}\Big(c_1(s-4m_\pi^2)^5 + c_2(s-4m_\pi^2)^4 + c_3(s-4m_\pi^2)^3 + \\ + c_4(s-4m_\pi^2)^2 + c_5(s-4m_\pi^2) + c_6\Big)\,, \tag{39}$$

$$D_i(s) = m_i^2 - s - g_i\Pi_{\pi\pi}(s)\,, \tag{40}$$

$$\Pi_{\pi\pi}(s) = \frac{16\pi}{g_{Rab}^2}\Pi_R^{\pi\pi}(s)\,, \tag{41}$$

$$P_{\pi 1}^*(s) = P_{\pi 1}(s-i\epsilon) = P_{\pi 1}(s) + 2i\rho_{\pi\pi}(s)\Big(1 + a_4K_1(s)\Big)\,, \tag{42}$$

$$P_{\pi 2}(s) = \frac{\Lambda^2 + s - 4m_\pi^2}{4m_\pi^2} + k_2Q_2(s)\,, \tag{43}$$

here

$$Q_2(s) = \frac{1}{\pi}\int_{4m_\pi^2}^{\infty}\frac{s-4m_\pi^2}{s'-4m_\pi^2}\frac{\rho_{\pi\pi}(s')}{s'-s-i\varepsilon}K_2(s')\,, \tag{44}$$

$$K_2(s) = \frac{L_2(s)}{D_{1A}(4m_\pi^2-s)D_{2A}(4m_\pi^2-s)D_{3A}(4m_\pi^2-s)}\,, \tag{45}$$

$$L_2(s) = 4m_\pi^2\Big(s^2 + \beta s + \gamma_1 s^{3/2} + \gamma_2 s^{1/2}\Big)\,, \tag{46}$$

$$P_{\pi 2}^*(s) = P_{\pi 2}(s-i\epsilon) = P_{\pi 2}(s) - 2i\rho_{\pi\pi}(s)k_2K_2(s)\,. \tag{47}$$

Note that this parameterization was inspired by Ref. [19], devoted to proof that the propagators (8) satisfy the Källen – Lehmann representation in the wide domain of coupling constants of the scalar mesons with the two-particle states. Following the ideas of this paper the conditions

$$K_1(s) \geq 0,\ K_2(s) \geq 0 \text{ at } s > 4m_\pi^2$$

guarantee absence of poles on the physical sheet in Eq. (35) (of course, the restrictions of Sec. IV should be fulfilled too). Note also that we choose the denominator of (35) as $P_{\pi 1}(s)P_{\pi 2}(s)$ for our comfort.

IV. RESTRICTIONS ON THE PARAMETERS

Some parameters are fixed by the requirement of the proper analytical continuation of amplitudes. The denominators $P_{\pi 1}$ and $P_{\pi 2}$ have zeroes at $s = m_0^2$ and $s = m_{0A}^2$ respectively, both belonging to the interval $0 < s < 4m_\pi^2$. These zeroes should be compensated by zeroes in any pair from $P^*_{\pi 1}$, $P^*_{\pi 2}$ and $S_0^{0\ res}$. We choose

$$P^*_{\pi 1}(m_0^2) = 0\,,$$

$$S_0^{0\ res}(m_{0A}^2) = 0 \tag{48}$$

see Eq. (35). [28]

The requirement of the T_0^0 finitness at $s = 0$ leads to 2 conditions. Really, on the real axis for $s > 4m_\pi^2$ we have

$$S_1^{back} = \frac{P^*_{\pi 1}(s)}{P_{\pi 1}(s)} = \frac{P_{\pi 1}(s - i\epsilon)}{P_{\pi 1}(s + i\epsilon)} = 1 + 2i\rho_{\pi\pi}(s)\frac{1 + K_1(s)}{P_{\pi 1}(s)}\,,$$

$$S_2^{back} = \frac{P^*_{\pi 2}(s)}{P_{\pi 2}(s)} = \frac{P_{\pi 2}(s - i\epsilon)}{P_{\pi 2}(s + i\epsilon)} = 1 - 2i\rho_{\pi\pi}(s)\frac{K_2(s)}{P_{\pi 2}(s)}\,.$$

So, to avoid singularity in the

$$T_0^0 = \frac{S_1^{back}S_2^{back}S_0^{0\,res} - 1}{2i\rho_{\pi\pi}(s)}$$

at $s = 0$, where $\rho_{\pi\pi}(s)$ becomes infinite, we require

$$1 + K_1(0) = 0,$$

as for $K_2(0)$, it is equal to zero at $s = 0$ via construction, see Eq. (45). Note that alternatively one may require $T_0^{0\,res}(0) = 0$.

Additionally, as it was noted in Refs. [29], crossing symmetry implemented by Roy equations imposes the condition

$$\frac{dT_0^0}{dm}(m^2=0)=0\,.$$

Remain also the condition Eq. (30) removing the singularity in the $T(\pi\pi \to K\bar{K})$ amplitude. One can see that no special prerequisite to Adler zero existence in the $\pi\pi$ scattering amplitude should be imposed, because it appears when we take into account the results of Ref. [6].

V. DATA ANALYSIS

Analyzing data we imply a scenario motivated by the four-quark model [30], that is, the $\sigma(600)$ coupling with the $K\bar{K}$ channel, $g_{\sigma K^+K^-}$, is suppressed relatively to the coupling with the $\pi\pi$ channel, $g_{\sigma\pi^+\pi^-}$, the mass of the σ meson m_σ is in the 500-700 MeV range. In addition, we have in mind the Adler self-consistency conditions for the $T_0^0(\pi\pi \to \pi\pi)$ near $\pi\pi$ threshold. The general aim of this section is to demonstrate that the data and the [6] results on the $\pi\pi$ amplitude are in excellent agreement with this general scenario.

As in Ref. [2] for $\phi \to \pi^0\pi^0\gamma$ decay we use the KLOE data [3] for $m > 660$ MeV. For the δ_0^0 we use the "old data" [31–35], 44 points up to 1.2 GeV [36]. Besides, we take into account the new precise data in the low energy region [37, 38].

The inelasticity $\eta_0^0(m)$ and the phase $\delta^{\pi K}(m)$ of the amplitude $T(\pi\pi \to K\bar{K})$ are essential in the fit region, $2m_{K^+} < m < 1.2$ GeV. As for the inelasticity, the experimental data of Ref. [31] gives an evidence in favor of low values of $\eta_0^0(m)$ near the $K\bar{K}$ threshold. The situation with the experimental data on $\delta^{\pi K}(m)$ is controversial and experiments have large errors. We consider these data as a guide, which main role is to fix the sign between signal (4) and background amplitudes (3), and hold two points of the experiment [39], see Fig. 9. As for inelasticity, for fitting we used only the key experimental point $\eta_0^0(m = 1.01\ \text{GeV}) = 0.41 \pm 0.14$, see Fig. 5.

Providing all the above conditions, we have obtained perfect agreement with the general scenario under consideration, see Fits 1, 2 in Tables I, II and Figs. 1-10. Fits 1 and 2 show that allowed range of $\sigma(600)$ and $f_0(980)$ parameters is rather wide.

The values of $g^2_{f_0K^+K^-}/4\pi$ in Fits 1 and 2 (1 GeV^2 and 2 GeV^2 correspondingly) show scale of possible deviation of this constant. This may be important to coordinate $g^2_{f_0K^+K^-}/4\pi$ with $g^2_{a_0K^+K^-}/4\pi$ [40], note the latter is usually larger than 1 GeV^2.

In addition, we carry out Fit 3, where $\sigma(600)$ and $f_0(980)$ are coupled only with the $\pi\pi$ channel. As seen from Table I and Figs. 11-13, Fit 3 is in excellent agreement with the data on the δ_0^0 up to 1 GeV and the [6] results.

We introduce rather many parameters indeed (52), but for restrictions (expresses 5 parameters through others) and parameters (or their combinations), that go to bound of the permitted range (7 effective links), the effective number of free parameters is reduced (to 40). It is significant that fits describe not only the experimental data (about 80 points), but also the $\pi\pi$ amplitude from the [6] in the range $-5m_\pi^2 < s < 0.64$ GeV^2 which is treated along with experimental data.

The $\sigma(600)$ pole positions, obtained in Fits 1 and 2, lie far from Eq. (1), see Table I. One of the possible reasons is neglecting $K\bar{K}$ and other high channels in the [6] approach. The role of high channels can be estimated with the help of Fit 3, which $\sigma(600)$ pole position is considerably closer to Eq. (1), see Table I.

Note that kernels of the background integrals (38) and (45) are positive in the range of integration $[2m_\pi, \infty)$, Fit 1 kernels are presented in Fig. 7.

The Adler zero in the $T_0^0(\pi\pi \to \pi\pi)$ is near $s = (100\ \text{MeV})^2$ in all Fits because we describe the amplitude [6]. Fit 2 also has Adler zero in the $T(\pi\pi \to K\bar{K})$ at $s = (166\ \text{MeV})^2$, Fit 1 has a zero in the $T(\pi\pi \to K\bar{K})$ at $s = -(601\ \text{MeV})^2$.

The resonance amplitude $T_0^{0\,res}$ have poles on the unphysical sheets of its Riemannian surface. As we have multi-channel case, the amplitude has the set of lists depending on lists of the polarization operators $\Pi_R^{ab}(s)$. We show resonance poles only on some lists, see Tables IV, V. For this choice, in case of metastable states, decaying to several channels, the imaginary parts of pole positions M_R would be connected to the full widths of the resonances ($2\text{Im}M_R = \Gamma_R = \sum_{ab}\Gamma(R \to ab)$). Note that $\sigma(600)$ and $f_0(980)$ poles, shown in Table I, correspond to first lines of Tables IV, V.

As to the background amplitude $T_0^{0\,back}$, it has poles on the second sheet of the Riemannian surface, where $P_{\pi 1} = 0$ or $P_{\pi 2} = 0$. The $P_{\pi 1}$ has a zero at $s = (1246 - 104\,i)^2$ MeV^2 for Fit 1, at $s = (1354 - 110\,i)^2$ MeV^2 for Fit 2, and at $s = (1056 - 142\,i)^2$ MeV^2 for Fit 3. The $P_{\pi 2}$ has a zero at $s = (0.2 - 9.5\,i)\,m_\pi^2$ for Fit 1, at $s = (2.0 - 8.9\,i)\,m_\pi^2$ for Fit 2, and at $s = (-0.6 - 8.6\,i)\,m_\pi^2$ for Fit 3. These poles lie outside of the region $4m_\pi^2 < \text{Re}(s) < (1.2$ GeV$)^2$ except the pole at $s = (1056 - 142\,i)^2$ MeV^2 for Fit 3, but for this Fit the upper bound is 1 GeV^2.

Note it would be naive to treat the poles in the background as resonances ($f_0(1370)$, for example) because in our approach to consider additional resonances one should extend the matrix of the inverse propagators, etc.

Table I. Properties of the resonance amplitude and main characteristics

Fit	1	2	3
m_{f_0}, MeV	979.16	986.50	964.01
$g_{f_0K^+K^-}$, GeV	3.54	5.01	0
$\frac{g^2_{f_0K^+K^-}}{4\pi}$, GeV^2	1	2	0
$g_{f_0\pi^+\pi^-}$, GeV	-1.3737	-2.1185	0.3183
$\frac{g^2_{f_0\pi^+\pi^-}}{4\pi}$, GeV^2	0.150	0.357	0.008
x_{f_0}	0.6640	0.9584	-
$\Gamma_{f_0}(m_{f_0})$, MeV	55.2	130.3	3.0
$f_0(980)$ pole, MeV	$986.2 - 25.5\,i$	$990.5 - 19.4\,i$	$978.9 - 11.4\,i$
m_σ, MeV	487.59	506.95	480.46
$g_{\sigma\pi^+\pi^-}$, GeV	2.7368	2.6735	2.5871
$\frac{g^2_{\sigma\pi^+\pi^-}}{4\pi}$, GeV^2	0.596	0.569	0.533
$g_{\sigma K^+K^-}$, GeV	0.552	0.774	0
$\frac{g^2_{\sigma K^+K^-}}{4\pi}$, GeV^2	0.024	0.048	0
x_σ	0.9750	0.8201	-
$\Gamma_\sigma(m_\sigma)$, MeV	377.8	352.9	340.2
$\sigma(600)$ pole, MeV	$581.0 - 212.7\,i$	$613.8 - 221.4\,i$	$528.6 - 220.3\,i$
C, GeV^2	0.04317	-0.07633	-0.11734
δ, $^\circ$	-70.62	-73.6	-
m_1, MeV	801.90	814.88	-
m_2, MeV	465.95	554.95	-
Λ_K, GeV	1.142	1.030	-
$a_0^0,\ m_\pi^{-1}$	0.223	0.226	0.221
Adler zero in $\pi\pi \to \pi\pi$	(94.4 MeV)^2	(96.8 MeV)^2	(87.1 MeV)^2
η_0^0(1010 MeV)	0.55	0.45	-
χ^2_{phase} (44 points)	45.9	50.6	26.3 (34 points)
χ^2_{sp} (18 points)	24.9	19.1	-

Table II. Parameters of the first background ($P_{\pi 1}$)

Fit	1	2	3
a_1	-3.105	-4.549	-1.498
a_2	0.01136	0.00998	0.05821
a_3	0	0	0
a_4	4.9328	13.1111	1.2475
α_1, GeV^2	604.137	624.512	-792.804
α_2, GeV^4	920.111	1000.739	-384.477
α_3, GeV^6	785.958	781.770	416.645
α_4, GeV^8	223.623	211.195	198.772
α_5, GeV^{10}	24.5339	23.8517	25.4265
α_6, GeV^{12}	0.248657	0.314094	0.198560
c_1, GeV	356.128	224.404	995.905
c_2, GeV^3	-2735.40	-2600.82	-1070.75
c_3, GeV^5	284.008	445.192	542.745
c_4, GeV^7	430.758	461.717	411.927
c_5, GeV^9	49.7913	47.2357	51.4206
c_6, GeV^{11}	-0.664290	-0.684002	-0.635647
m_1, MeV	1105.67	1111.87	1002.31
g_1, MeV	347.70	350.48	306.18
m_2, MeV	1061.53	1141.92	806.93
g_2, MeV	344.12	381.73	350.51
m_3, MeV	1061.85	1169.51	781.76
g_3, MeV	311.56	311.80	322.57
m_4, MeV	970.78	1040.96	970.78
g_4, MeV	457.52	455.56	376.88
m_5, MeV	1176.39	1320.55	1153.21
g_5, MeV	544.43	588.48	500.59
m_6, MeV	1521.20	1621.10	1808.74
g_6, MeV	739.93	750.75	841.57

Table III. Parameters of the second background ($P_{\pi 2}$)

Fit	1	2	3
Λ, MeV	83.238	74.477	70.268
k_2	0.0152934	0.0168176	0.0150655
β	239.184	221.055	263.511
γ_1	1006.367	928.743	878.056
γ_2	22.7004	23.3341	29.4097
m_{1A}, MeV	491.92	84.77	687.43
g_{1A}, MeV	469.29	492.03	364.68
m_{2A}, MeV	531.81	639.95	528.40
g_{2A}, MeV	452.20	261.48	378.65
m_{3A}, MeV	670.64	565.16	608.72
g_{3A}, MeV	299.23	428.97	370.98

Table IV. $\sigma(600)$ poles (MeV) on different sheets of the complex s plane depending on lists of polarization operators $\Pi^{ab}(s)$

$\Pi^{K\bar{K}}$ list	$\Pi^{\eta\eta}$ list	$\Pi^{\eta\eta'}$ list	$\Pi^{\eta'\eta'}$ list	Fit 1	Fit 2
I	I	I	I	$581.0 - 212.7\,i$	$613.8 - 221.4\,i$
II	I	I	I	$617.5 - 353.0\,i$	$609.8 - 291.6\,i$
II	II	I	I	$554.3 - 375.3\,i$	$559.4 - 346.6\,i$
II	II	II	I	$579.0 - 475.2\,i$	$569.7 - 410.7\,i$
II	II	II	II	$625.7 - 474.9\,i$	$581.6 - 411.0\,i$

Table V. $f_0(980)$ poles (MeV) on different sheets of the complex s plane depending on lists of polarization operators $\Pi^{ab}(s)$

$\Pi^{K\bar{K}}$ list	$\Pi^{\eta\eta}$ list	$\Pi^{\eta\eta'}$ list	$\Pi^{\eta'\eta'}$ list	Fit 1	Fit 2
I	I	I	I	$986.2 - 25.5\,i$	$990.5 - 19.4\,i$
II	I	I	I	$916.9 - 299.4\,i$	$1183.2 - 518.6\,i$
II	II	I	I	$966.8 - 450.5\,i$	$1366.0 - 756.5\,i$
II	II	II	I	$962.6 - 465.2\,i$	$1390.7 - 813.0\,i$
II	II	II	II	$962.5 - 608.0\,i$	$1495.6 - 1057.7\,i$

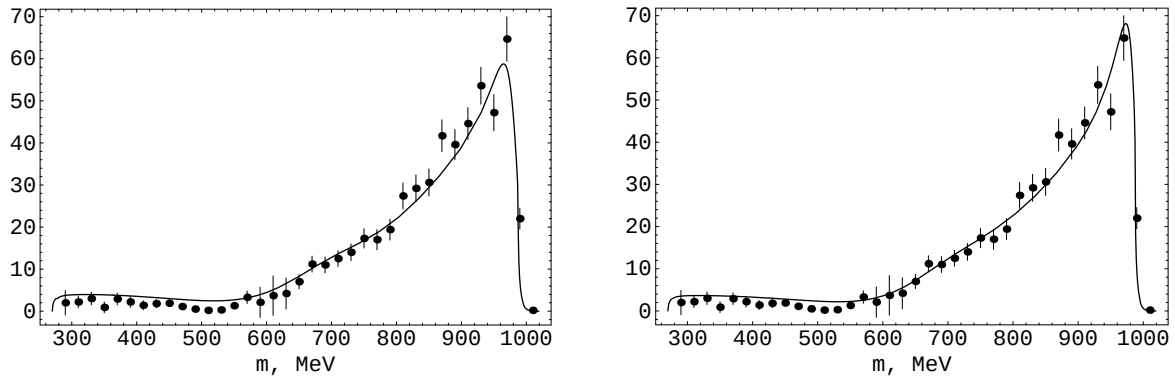

(a) (b)

FIG. 1: The $\pi^0\pi^0$ spectrum, theoretical curve and the KLOE data (points): a) Fit 1, b) Fit 2.

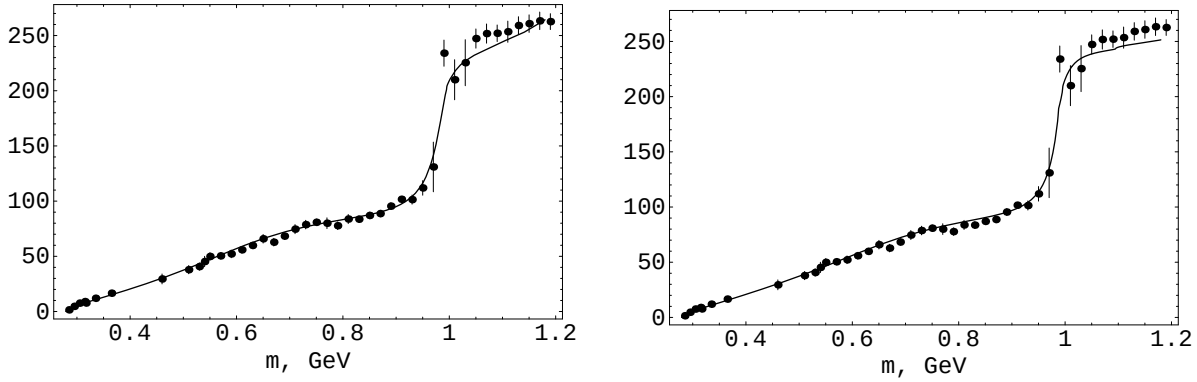

(a) (b)

FIG. 2: The phase δ_0^0 of the $\pi\pi$ scattering (degrees): a) Fit 1, b) Fit 2.

VI. CONCLUSION

Thus, the background phase (34) allows us to obtain proper analytical features of the $\pi\pi$ scattering amplitude, link results of [6] with properties of light scalars simultaneously describing experimental data. The obtained description is in agreement with the scenario based on the four-quark model.

Resonance masses and widths m_R and $\Gamma_R(m_R)$ in our formulas (which may be called "Breit-Wigner" masses and widths) have clear physical meaning, in contrast to the resonance poles in the complex plane. At first, what sheet of the complex plane should be considered?

For $\sigma(600)$ it is natural to consider the first line of the Table IV (at any rate, it would be correct for very narrow $\sigma(600)$). The obtained pole positions in this case don't agree with

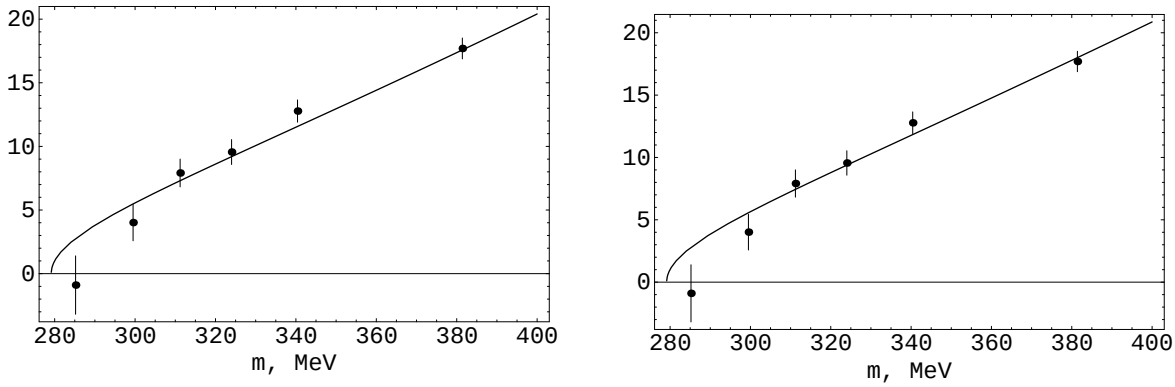

(a) (b)

FIG. 3: The comparison of the experimental data on δ_0^0 [37] and the obtained curve: a) Fit 1, b) Fit 2.

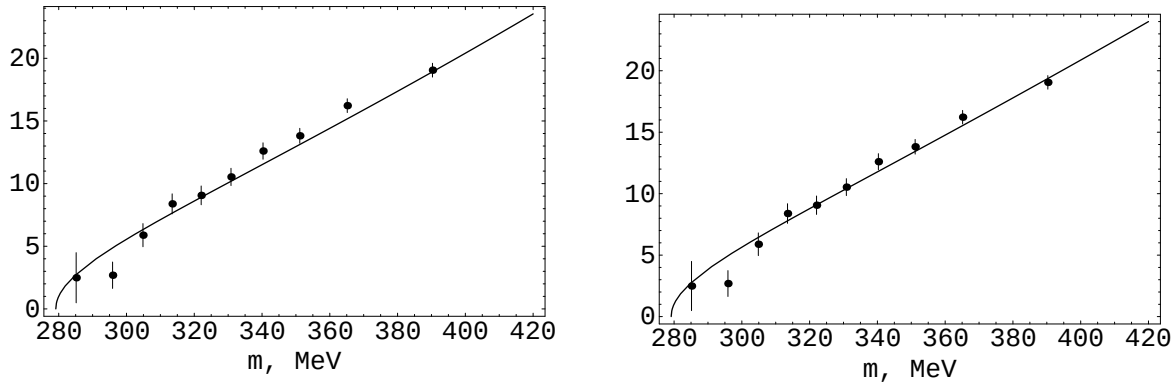

(a) (b)

FIG. 4: The comparison of the experimental data on δ_0^0 [38] and the obtained curve: a) Fit 1, b) Fit 2.

the pole position obtained in Ref. [6], see Eq. (1). Note that the $\sigma(600)$ pole position is dictated by the $\sigma(600)$ propagator in our case, because the $\sigma(600) - f_0(980)$ mixing is small. Providing the pole position (1) and taking into account only $\pi\pi$ channel in the propagator, we can determine $\sigma(600)$ mass and coupling to the $\pi\pi$ channel, and the obtained values contradict the Källen – Lehmann representation, see [19]. Taking into account additional channels we may fulfill the Källen – Lehmann representation, but the region of permitted $\sigma(600)$ parameters don't allow to describe experimental data in the current model.

Note that the Roy equations are approximate, they take into account only $\pi\pi$ channel. This can lead to different analytical continuation and, hence, explain deviation of the $\sigma(600)$

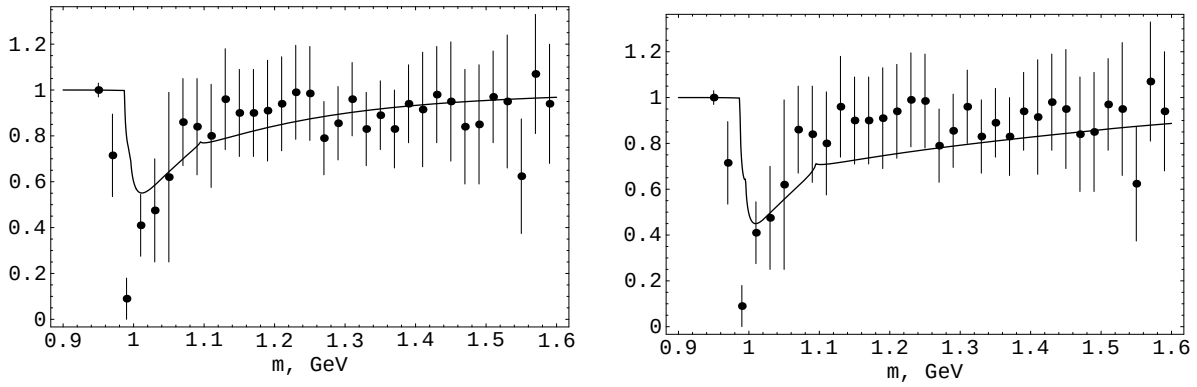

(a) (b)

FIG. 5: The inelasticity η_0^0: a) Fit 1, b) Fit 2.

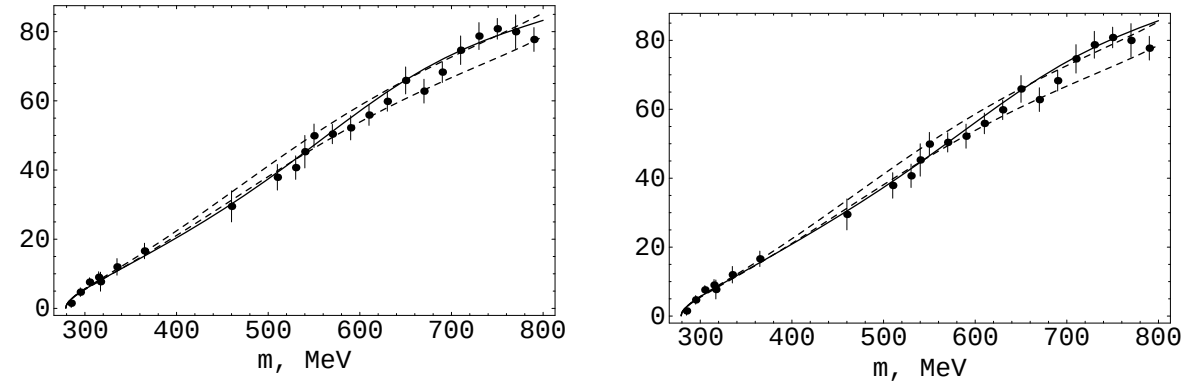

(a) (b)

FIG. 6: The phase δ_0^0 of the $\pi\pi$ scattering. Solid line is our description, dashed lines mark borders of the corridor [6], points are experimental data: a) Fit 1, b) Fit 2.

pole position, compare Fit 3 with Fits 1 and 2 in Table I [42].

The current activity, aiming extremely precise determination of the $\sigma(600)$ pole position, has taken the forms of the Swift's grotesque. Really, the residue of the σ pole can not be connected to coupling constant in the Hermitian (or quasi-Hermitian) Hamiltonian, see Ref. [5], for it has a large imaginary part and this pole can not be interpreted as a physical state for its huge width.

The futility of the approach basing on poles treatment may be additionally illustrated by Fit 2. As seen on line 1 of Table V, real part of the $f_0(980)$ pole ReM_{f_0} on the II sheet of the T_0^0 exceeds the K^+K^- threshold (987.4 MeV), it means that ImM_{f_0} equals to

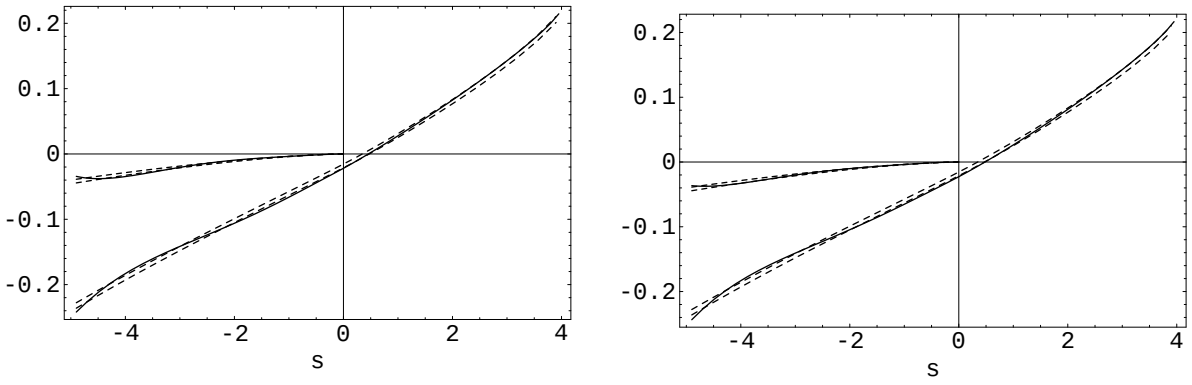

(a) (b)

FIG. 7: The real and the imaginary parts of the amplitude T_0^0 of the $\pi\pi$ scattering (s in units of m_π^2). Solid lines show our description, dashed lines mark borders of the real part corridor and the imaginary part for $s < 0$ [6]: a) Fit 1; b) Fit 2.

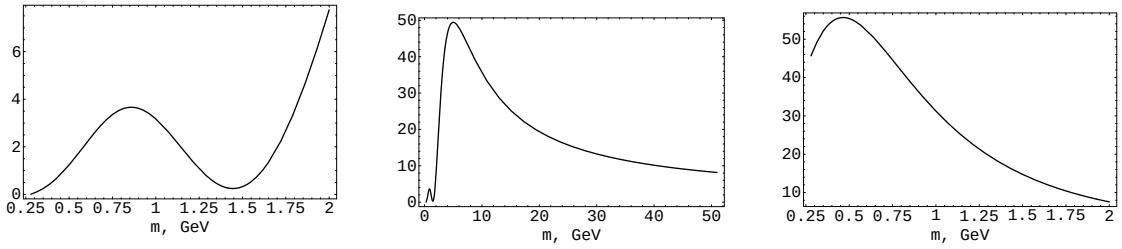

(a) (b) (c)

FIG. 8: Kernels $K_1(m^2)$ and $K_2(m^2)$ for Fit 1: a) $K_1(m^2)$ below 2 GeV. Minimum near 1.4 GeV is 0.25. b) $K_1(m^2)$ up to 50 GeV. Then it asymptotically tends to 1. c) $K_2(m^2)$ up to 2 GeV. Then it asymptotically tends to zero.

$-\Big(\Gamma(f_0(980)\to\pi\pi)-\Gamma(f_0(980)\to K^+K^-)\Big)/2$, what is physically meaningless. In this case we should take $\Pi^{K^+K^-}$ from the second sheet, this gives the pole at $M_{f_0} = 989.6 - 168.7\,i$ MeV, with ReM_{f_0} between the K^+K^- and $K^0\bar{K^0}$ thresholds again. But as we work on the s plane, we should consider not M_{f_0}, but $M_{f_0}^2 = (0.951 - 0.334\,i)$ GeV^2. So we have the pole with real part below the K^+K^- and $K^0\bar{K^0}$ thresholds and imaginary part dictated by analytical continuation of the kaon polarisation operators.

To reduce an effect of heavier isosinglet scalars we restrict ourselves to the analysis of the mass region $m < 1.2$ GeV. As to mixing light and heavier isosinglet scalars, this question could not be resolved once and for all at present, in particular, because their properties are

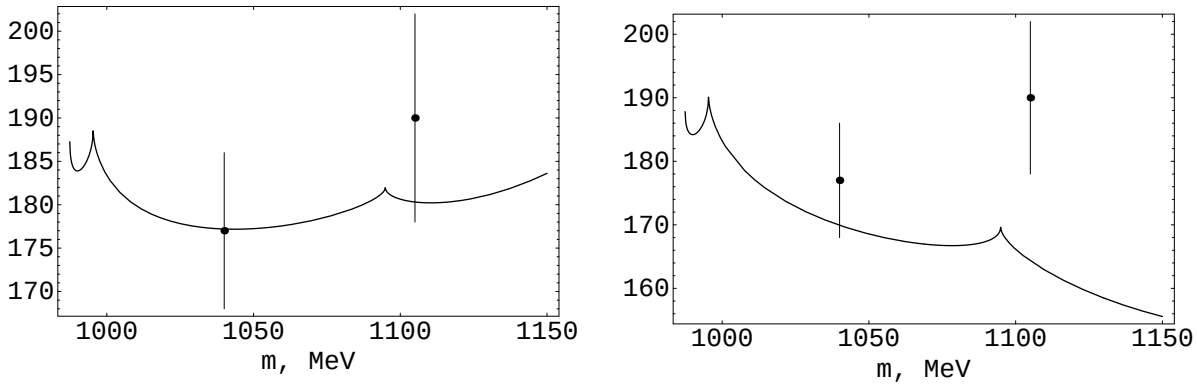

(a) (b)

FIG. 9: The phase $\delta^{\pi K}$ of the $\pi\pi \to K\bar{K}$ scattering

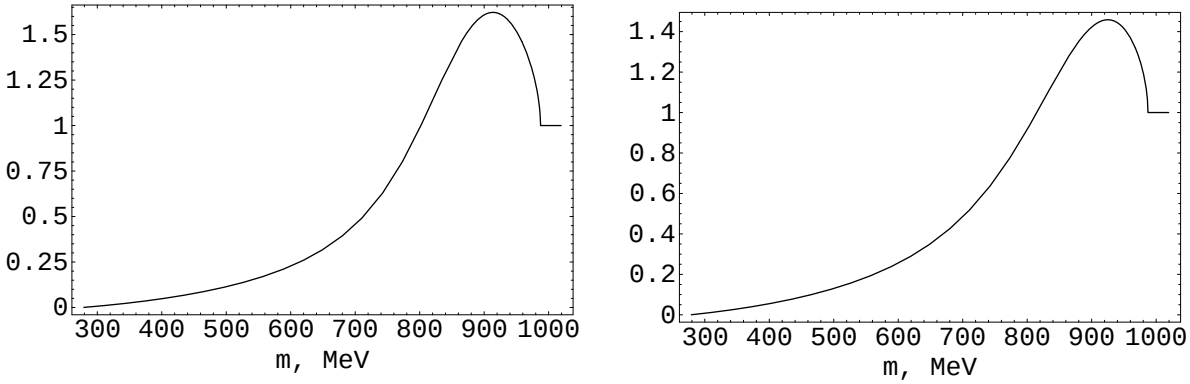

(a) (b)

FIG. 10: The $|P_K(m)|^2$, see Eq. (7).

not well-established up to now. A preliminary consideration was carried out in Ref. [43], where, in particular, it was shown that the mixing could affect the mass difference of the isoscalar and isovector.

The factor $|P_K(s)|^2$ modifying the $|T(\pi\pi \to K\bar{K})|^2$, see Eqs. (7) and (31), is shown on Fig. 10. This factor don't change the Kaon Loop Model radically, but helps to fulfill the requirement (30) and to improve the data description. The influence of this factor may be reduced if to use a more skilful form than Eq. (31) for it.

New precise experimental data are needed for the investigation of light scalars. The elucidation of the situation, a contraction of the possible variants or even the selection of the unique variant, requires considerable efforts. The new precise experiment on $\pi\pi \to K\bar{K}$

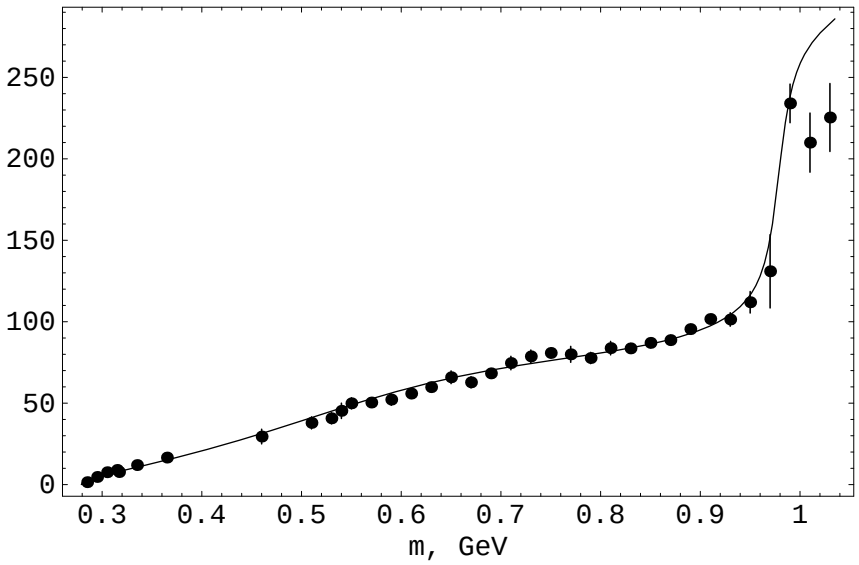

FIG. 11: The phase δ_0^0 of the $\pi\pi$ scattering, Fit 3 and the experimental data.

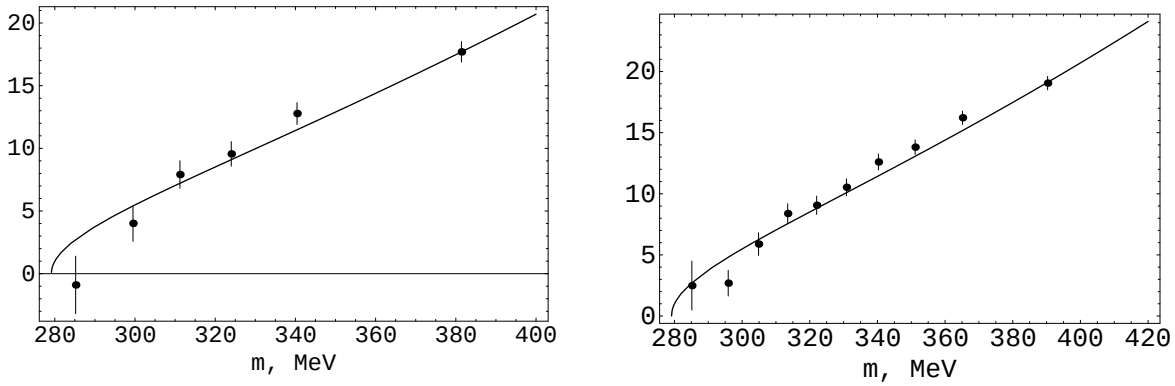

(a) (b)

FIG. 12: The phase δ_0^0 of the $\pi\pi$ scattering, Fit 3. The comparison with the data a) [37], b) [38].

would give the crucial information about the inelasticity η_0^0 and about the phase $\delta_B^{K\bar{K}}(m)$ near the $K\bar{K}$ threshold. The forthcoming precise experiment in KLOE on the $\phi \to \pi^0\pi^0\gamma$ decay will also help to judge about this phase in an indirect way. The precise measurement of the inelasticity η_0^0 near 1 GeV in $\pi\pi \to \pi\pi$ would be very important also.

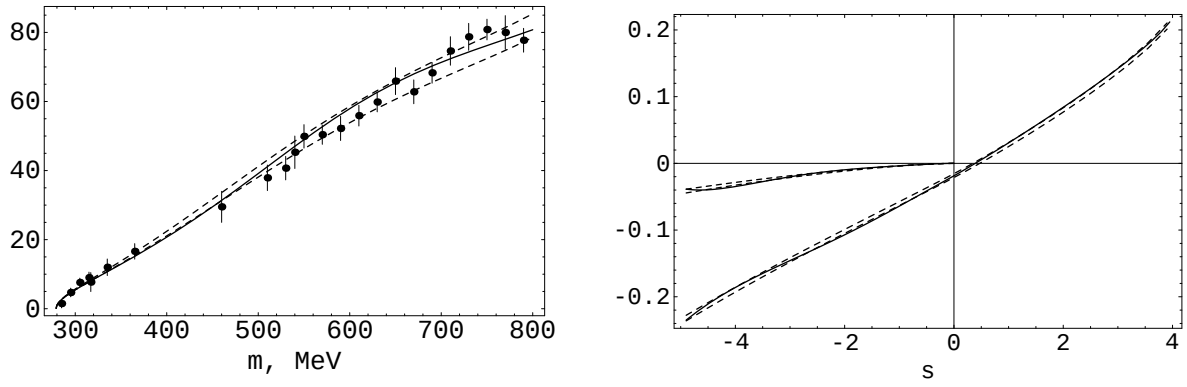

(a) (b)

FIG. 13: a) The phase δ_0^0 of the $\pi\pi$ scattering, Fit 3. Solid line is our description, dashed lines mark borders of the corridor [6], points are experimental data. b) The real and the imaginary parts of the amplitude T_0^0 of the $\pi\pi$ scattering (s in units of m_π^2). Solid lines correspond to Fit 3, dashed lines mark borders of the real part corridor and the imaginary part for $s < 0$ [6].

VII. ACKNOWLEDGEMENTS

We thank very much H. Leutwyler for providing numerical values of the $T_0^0(s)$ on the real axis, obtained in Ref. [6], useful discussions and kind contacts. This work was supported in part by RFBR, Grant No 10-02-00016.

[1] Particle Data Group-2008, C. Amsler et al., Phys. Lett. **B667**, 1 (2008).

[2] N.N. Achasov, A.V. Kiselev, Phys. Rev. **D73**, 054029 (2006); Erratum-ibid. **D74**, 059902 (2006); Yad. Fiz. **70**, 2005 (2007) [Phys. At. Nucl. **70**, 1956 (2007)].

[3] KLOE Collaboration, A.Aloisio et al., Phys. Lett. **B537** (2002).

[4] N.N. Achasov and G.N. Shestakov, Phys. Rev. **D49**, 5779 (1994); Yad.Fiz. **56**, 206 (1993) [Phys. At. Nucl. **56**, 1270 (1993)]; Int. J. Mod. Phys. **A9**, 3669 (1994).

[5] N.N. Achasov and G.N. Shestakov, Phys. Rev. Lett. **99**, 072001 (2007).

[6] I. Caprini, G. Colangelo and H. Leutwyler, Phys. Rev. Lett. **96**, 132001 (2006).

[7] S.L. Adler, Phys. Rev. **B137**, 1022 (1965); ibid. **B139**, 1638 (1965).

[8] We met the opinion that the representation (2) violates analiticity, because the amplitude

$$T_{\pi\pi} = T_{res} + T_{back} + 2i\rho_{\pi\pi} T_{res} T_{back}$$

becomes infinite at $s \to \infty$ for $\rho_{\pi\pi} = \sqrt{1 - 4m_\pi^2/s} \to \infty$. This obstacle may be overcome if T_{res} or T_{back} is equal to zero at $s = 0$. As in Ref. [2], we choose here the second variant, $T_{back}(0) = 0$.

[9] N.N. Achasov and V.N. Ivanchenko, Nucl. Phys. **B315**, 465 (1989); Preprint INP 87-129 (1987) Novosibirsk.

[10] N.N. Achasov and V.V. Gubin, Phys. Rev. **D56**, 4084 (1997); Yad. Fiz. **61**, 274 (1998) [Phys. At. Nucl. **61**, 224 (1998)].

[11] N.N. Achasov, V.V. Gubin, Phys. Rev. **D63**, 094007 (2001); Yad. Fiz. **65**, 1566 (2002) [Phys. At. Nucl. **65**, 1528 (2002)].

[12] N.N. Achasov and A.A. Kozhevnikov, Phys. Rev. **D61**, 054005 (2000); Yad. Fiz. **63**, 2029 (2000) [Phys. At. Nucl. **63**, 1936 (2000)].

[13] F_b may be considerably less than 1 due to the $\pi^0\pi^0$ final state interaction.

[14] N.N. Achasov, S.A. Devyanin, and G.N. Shestakov, Phys. Lett. **96B**, 168 (1980).

[15] N.N. Achasov, S.A. Devyanin, and G.N. Shestakov, Yad. Fiz. **32**, 1098 (1980)[Sov. J. Nucl. Phys. **32**, 566 (1980)].

[16] N.N. Achasov, S.A. Devyanin and G.N. Shestakov, Z. Phys. **C22**, 53 (1984);

[17] N.N. Achasov, S.A. Devyanin and G.N. Shestakov, Usp. Fiz. Nauk. **142**, 361 (1984) [Sov. Phys. Usp. **27**, 161 (1984)].

[18] N.N. Achasov, S.A. Devyanin, and G.N. Shestakov, Phys. Lett. **88B**, 367 (1979).

[19] N.N. Achasov and A.V. Kiselev, Phys. Rev. **D70**, 111901 (R) (2004).

[20] N.N. Achasov, *THE SECOND DAΦNE PHYSICS HANDBOOK*, Vol. II, edited by L. Maiani, G. Pancheri, N. Paver, dei Laboratory Nazionali di Frascati, Frascati, Italy (May 1995), p. 671.

[21] N.N. Achasov and G.N. Shestakov, Usp. Fiz. Nauk. **161** (6), 53 (1991)[Sov. Phys. Usp. **34** (6), 471 (1991)]; N.N. Achasov, Nucl. Phys. B (Proc. Suppl.) **21**, 189 (1991); N.N. Achasov, Usp. Fiz. Nauk. **168**, 1257 (1998) [Phys. Usp. **41**, 1149 (1998)]; N.N. Achasov, Nucl. Phys. **A675**, 279c (2000).

[22] N.N. Achasov and V.V. Gubin, Phys. Rev. **D64**, 094016 (2001); Yad. Fiz. **65**, 1939 (2002)

[Phys. At. Nucl. **65**, 1887 (2002)].

[23] N.N. Achasov and A.V. Kiselev, Phys. Rev. **D68**, 014006 (2003); Yad. Fiz. **67**, 653 (2004) [Phys. At. Nucl. **67**, 633 (2004)].

[24] M.N. Achasov et al, Phys. Rev. **D63**, 072002 (2001).

[25] S.I. Dolinsky et al., Z. Phys. **C42**, 511 (1989).

[26] M.N. Achasov et al, Phys. Lett. **B559**, 171 (2003).

[27] Note that in general the existence of Adler zero in partial amplitudes is not obligatory, see APPENDIX II in Ref. [2].

[28] Note that the condition (48) is similar to the condition (34) in PRD of Ref. [2] (in Phys. At. Nucl. it is (36)).

[29] I. Caprini, Phys.Rev. **D** 77, 114019 (2008);
G. Colangelo, J. Gasser and H. Leutwyler, Nucl. Phys. B 603 125 (2001).

[30] R.L. Jaffe, Phys. Rev. **D15**, 267, 281 (1977).

[31] B. Hyams et al., Nucl. Phys. **B64**, 134 (1973).

[32] P. Estabrooks and A.D. Martin, Nucl. Phys. **B79**, 301 (1974).

[33] A.D. Martin, E.N. Ozmutlu, E.J. Squires, Nucl. Phys. **B121**, 514 (1977).

[34] V. Srinivasan et al., Phys. Rev. **D12**, 681 (1975).

[35] L. Rosselet et al., Phys. Rev. **D15**, 574 (1977).

[36] The same data was used in [2], but only up to 1.1 GeV. We add the data up to 1.2 GeV to provide better behaviour of our δ_0^0 and inelasticity, considering influence of high-energy resonances smaller than experimental errors.

[37] S. Pislak et al., Phys. Rev. Lett. **87** 221801 (2001).

[38] J.R. Batley et al., Eur. Phys. J. **C54**, 411 (2008).

[39] A. Etkin et al, Phys. Rev. **D25**, 1786 (1982).

[40] These constants are equal in the naive four-quark model.

[41] Taking into account that the $\sigma(600) - f_0(980)$ mixing is small.

[42] In addition, propagators (8) are approximate, and their small difference with "real" propagators in the physical region could be important in the complex s plane.

[43] D. Black, A. Fariborz, and J. Schechter, Phys. Rev. **D61** 074001 (2000).